ACS OMEGA

Open Access

http://pubs.acs.org/journal/acsodf

Article

Differentially Charged Liposomes Stimulate Dendritic Cells with Varying Effects on Uptake and Processing When Used Alone or in Combination with an Adjuvant

Mithun Maji, Sneha Ghosh, Nicky Didwania, and Nahid Ali*

Cite This: *ACS Omega* 2024, 9, 29175−29185

Read Online

ACCESS | Metrics & More | Article Recommendations

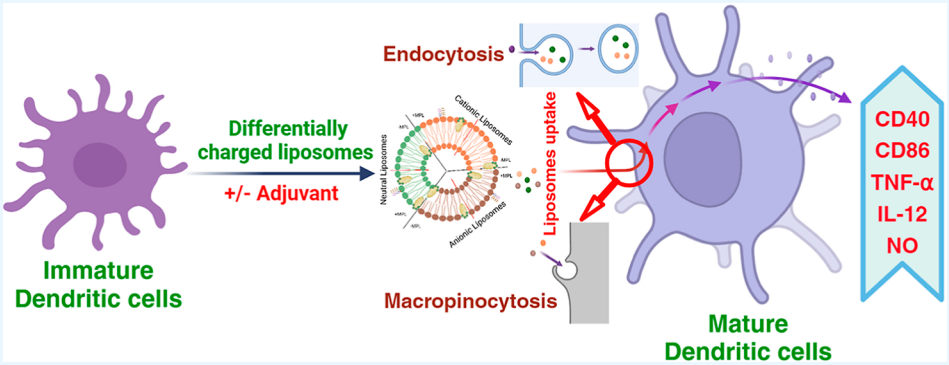

ABSTRACT: Liposomes carrying differential charges have been extensively studied for their role in stimulating dendritic cells (DCs), major antigen-presenting cells, known to serve as a pivotal bridge between innate and adaptive immunity. However, the impact of the differentially charged liposomes on activating DCs remains to be understood. In this study, we have investigated the impact of 1,2-distearoyl-*sn*-glycero-3-phosphocholine (DSPC)-based neutral, anionic, and cationic liposomes on the uptake, immunostimulation, and intracellular fate in mouse bone-marrow-derived DCs. We observed that liposomes could induce phenotypic maturation of DCs by inducing the expression of costimulatory molecules (CD40 and CD86) and production of cytokines tumor necrosis factor-α, interleukin-12,and nitric oxide. Interestingly, admixing monophosphoryl lipid A with charged liposomes further enhances the expression of the costimulatory molecules and production of cytokines, with preferential activation by positively charged liposomes. Fluorometric analysis using a pH-sensitive dye and flow-cytometry-based pathway inhibition assays revealed that cationic liposomes were taken up more efficiently by DCs through endocytosis and transported to neutral compartments for further processing, whereas anionic and neutral liposomes were inclined to accumulate in acidic compartments. These findings therefore endorse the use of cationic DSPC liposomes as a preferred option for vaccine delivery vehicles over neutral and negatively charged liposomes, particularly for the preferential activation of DCs.

INTRODUCTION

Vaccination remains the preeminent and cost-effective approach for preventing a spectrum of diseases globally. Although conventional whole-organism immunizations, such as the poliovirus vaccine, have achieved significant success in disease control and eradication, the emergence of novel vaccination strategies has introduced new avenues for enhancing efficacy and safety.[1] Recent advancements have seen the widespread acceptance of alternative vaccine technologies, including subunit antigens and recombinant nucleic acid approaches.[2] However, while these next-generation vaccines offer improved safety profiles compared to those of traditional methods, a key challenge persists: eliciting robust immunogenicity. This challenge arises from the removal of pathogenic characteristics in these newer approaches, necessitating innovative solutions to induce strong immune responses.[3]

Central to the advancement of subunit vaccines is the development of effective delivery systems and potent adjuvants. The efficacy of these vaccines relies not only on the delivery of antigens but also on their efficient uptake by antigen-presenting cells (APCs) and subsequent activation of immune responses.[4,5] Adjuvants play a critical role in

Received: October 7, 2023
Revised: January 8, 2024
Accepted: February 5, 2024
Published: June 25, 2024

https://doi.org/10.1021/acsomega.3c07814
ACS Omega 2024, 9, 29175−29185

augmenting immunogenicity by enhancing antigen presentation and stimulating the innate immune system through specific cell receptors.[6] While numerous adjuvants and delivery systems have been explored, the majority are yet to gain approval for human use due to safety concerns, leaving a significant gap in the search for effective and safe adjuvant systems.[7] Thus, there is an unmet need for an effective and safe adjuvant system that elicits both humoral and cellular immunity. Consequently, this advancement is poised to boost the effectiveness of vaccines, particularly in combating a range of critical bacterial infections such as tuberculosis, as well as viral pathogens like human immunodeficiency virus, Zika, and COVID-19. These are areas where either no viable vaccines exist or current vaccines have shown limited efficacy. This progress also holds promise in developing vaccines against challenging targets like tumors and cancers.[8]

In the realm of vaccine development, the quest for efficacious and safe delivery systems has led to the exploration of various innovative approaches. Among these, liposomes, lipid-based nanoparticles, have garnered significant attention as promising delivery vehicles, which modulate immunological responses.[9] Liposomes, characterized by biodegradable phospholipid bilayer membranes encapsulating aqueous compartments, have garnered attention for their compatibility (to entrap plasmid DNA, protein, and/or peptides), high encapsulation efficiency, and capacity for surface modifications.[10] These attributes position liposomal formulations as promising candidates for enhancing vaccine efficacy. Their ability to form complexes with charged biomolecules makes them particularly attractive for antigen delivery.[9] Important aspects for vaccine development with lipid particulate formulations include extended antigen delivery at the injection site and induced uptake via ionic interaction with a variety of charged membranous proteins of APCs.[11] Liposomes can also be used as an adjuvant to induce maturation and as a modulator of immunological responses, which is an added benefit of using these platforms.

The effect of adjuvanticity of liposomal formulations relies vastly upon the various physicochemical characteristics, such as lipid composition of the formulations, surface chemistry (electric charge), rigidity, size, and hydrophobicity.[12] Modifications in any of these physicochemical properties can lead to formulation-specific differential interaction behavior with immunological cells including APCs with a bona fide adjuvanticity.[13] Liposomal surface charge, in particular, plays an important role in uptake by APCs and is also a key factor in the T-cell-mediated immune regulatory effect of lipid-based nanoformulations.[14] Our previous findings have also indicated that liposomes with varying charges, when loaded with leishmanial antigen, produce distinct immunomodulatory effects. Notably, cationic liposomes (CLs) containing leishmanial antigen demonstrated substantial protection against experimental leishmaniasis.[15−17] Although these liposomal formulations demonstrated promising advantages as delivery vehicles, it has not been shown how the variation in liposomal charge impacts the uptake, immunostimulation, and intracellular fates in dendritic cells (DCs).

In light of these considerations, this study aims to elucidate the immunostimulatory potential of liposomal formulations with varying surface charges and their synergy with the adjuvant, monophosphoryl lipid A (MPL), and toll-like receptor (TLR)-4 agonist. Using bone-marrow-derived DCs (BMDCs), we investigate how differentially charged liposomes modulate DC maturation and activation, offering insights into their role in shaping effective vaccine strategies. In addition, we explore how the route of uptake by DCs changes with the charge of the vesicles. In summary, our study underscores the importance of the liposome surface charge in modulating the immunostimulatory activity of DCs. Furthermore, the synergy observed when MPL is combined with positively charged liposomes suggests exciting possibilities for the development of vaccines against life-threatening diseases.

MATERIALS AND METHODS

Animals. Bagg albino (BALB/c) mice (4−6 weeks old) were obtained from the CSIR-Indian Institute of Chemical Biology (CSIR-IICB, Kolkata, India) animal house. All mice were maintained in the institute's facilities under pathogen-free conditions with water and food given *ad libitum*. The mice were used for the experiment with prior approval from the Animal Ethics Committee of the IICB (147/1999/CPSCEA).

Preparation of Lipid Vesicles/Liposomes. Neutral, positive, and negatively charged liposomes were composed of DSPC and cholesterol (7:2 molar ratio), 1,2-distearoyl-*sn*-glycero-3-phosphocholine (DSPC), cholesterol, and either SA or phosphatidic acid (PA) (7:2:2 molar ratio), respectively. Briefly, lipids were dissolved in a methanol−chloroform solution, and the mixture was evaporated to dryness in a round-bottom glass flask to make a thin film and kept overnight in a desiccator at room temperature. The mixture was then vortexed after adding 0.02 M phosphate-buffered saline (PBS) and sonicated in an ultrasonicator (Misonix, New York, USA) for 30 s, followed by incubation at 4 °C for 2 h. Entrapment of a pH-sensitive, water-soluble fluorescent probe, pyranine (pyranine-8-hydroxypyrene-1,3,6-trisulfonic acid trisodium salt, Molecular Probes, USA) along with *p*-xylene-bis-pyridinium bromide (DPX, Molecular Probes, USA) was performed as described earlier.[18] To perform in vivo uptake studies, fluorescently labeled liposomes were formulated using the mentioned liposomal constituents, incorporating 0.1 mg/mL of rhodamine 123 as a lipophilic marker. The lipid film was dispersed in PBS, and unbound dye was removed from the labeled liposomes through centrifugation.

BMDC Culture. BMDCs were generated based on a previously reported method with some modifications (Inaba et al., 1992).[19] Briefly, bone marrow cells were cultured in a complete Roswell Park Memorial Institute (RPMI) 1640 medium supplemented with 15 ng/mL mouse recombinant granulocyte macrophage colony-stimulating factor (GM-CSF) and 10 ng/mL mouse recombinant interleukin (IL)-4. On day 4, non-adherent cells were removed, and adherent cells were cultured in a fresh medium containing GM-CSF and IL-4. Subsequently on day 6 or 7, immature DCs were incubated in fresh medium with different liposomal formulations (100 μM liposome concentration), lipopolysaccharide (LPS) 1 μg/mL, or monophosphoryl lipid-trehalose dimycolate (MPL-TDM) 100 ng/mL for 18−72 h at 37 °C in a humidified CO_2 (5%) incubator before analysis of tumor necrosis factor (TNF)-α, IL-12p40, and nitric oxide (NO) production and expression of surface costimulatory markers.

Measurement of Size and Zeta Potential. The mean diameter and zeta potential of the lipid vesicles were measured at room temperature by photon correlation spectroscopy by diluting the dispersion to the appropriate volume in doubly filtered (0.22 μm pore size) distilled water (Nano Zs ZetaSizer Malvern Instruments, Worcestershire, UK). The polydispersity

https://doi.org/10.1021/acsomega.3c07814
ACS Omega 2024, 9, 29175−29185

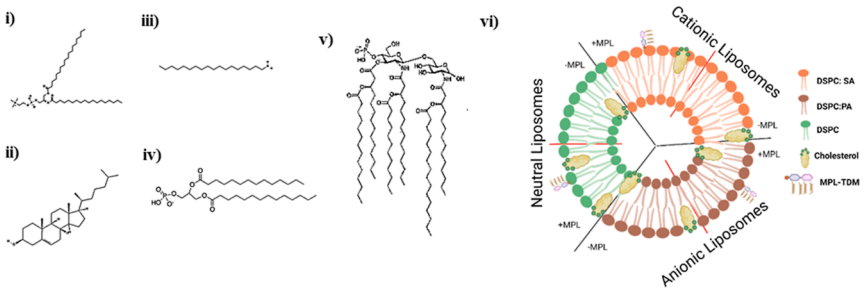

Figure 1. Schematic representation of differentially charged DSPC liposomes with their chemical structure and compositions. The neutral, positively, and negatively charged liposomes were made with DSPC and cholesterol or DSPC, cholesterol, and either SA or PA, respectively (for details, see the Material and Method section). Chemical structures of different lipid components used for preparation of variously charged liposomes. (i) DSPC, (ii) SA, (iii) Chol, (iv) PA, and (v) MPL. (vi) Schematic representation of different forms of liposome structure used in this study.

index (PDI) was used as a measure of the size distribution of the liposomes. A PDI value of 0.0 represents a homogeneous particle population, while a value of 1.0 indicates a heterogeneous liposome preparation.

Measurement of Cytokine Production. Mouse BMDCs were cultured and stimulated in vitro with medium alone or with different liposomal formulations for 18−24 h. The supernatants collected were stored at −70 °C for cytokine analysis. Measurement of TNF-α and IL-12 levels was carried out as detailed in the instructions supplied with the cytokine enzyme-linked immunosorbent assay (ELISA) kit (BD Biosciences, USA).

Measurement of NO Production. Culture supernatants of differentially stimulated BMDCs were collected and stored at −70 °C for the analysis of NO production. The accumulation of NO in the stimulated culture supernatants was measured as described previously.[20] Briefly, 50 μL of supernatants were mixed with an equal volume of Griess reagent (1% sulfanilamide and 0.1% *N*-1-naphthylethylene diamine hydrochloride in 50% H_3PO_4) and incubated at room temperature for 10 min. The absorbance was then measured at 540 nm in a plate reader (Thermo, Multiskan EX).

Flow Cytometric Assessment of DC Stimulation and Internalization of Liposomes with Varying Surface Charges. Differentially stimulated DCs were washed three times with PBS containing 0.5% bovine serum albumin and 0.1% NaN3 [fluorescence-activated cell sorting (FACS) buffer] to evaluate the surface expression of costimulatory molecules. After blocking with (phosphate buffered saline-fetal calf serum) PBS−FCS (1%), the cells were incubated for 30 min at 4 °C with fluorochrome-conjugated antibodies. The cells were then washed, suspended in PBS, and analyzed by flow cytometry (BD Biosciences, USA).

To evaluate the amount of cellular uptake of liposomes, BMDCs were incubated with rhodamine-123-labeled liposome in culture media (RPMI-1640 medium without FCS) for 1 h at 37 °C. In the inhibition experiment, before adding the various liposomes, DCs were incubated with amiloride (250 and 500 mol/L) or chlorpromazine (1 μg/mL and 5gμ/mL) for 30 min or 1 h. Following the incubation period, the cells were washed with PBS−FCS (0.5%) to remove surface-bound liposomes, and flow cytometric analysis (BD Bioscience, USA) was performed.

Bio-Distribution Study. Fluorescently labeled liposomes incorporating rhodamine 123 as a lipophilic marker (0.1 mg/mL) were used to investigate the biodistribution in BALB/c mice. Mice (n = 3) received intravenous injections of these labeled liposomes (80 μg/animal through tail vein) and were sacrificed 18−24 h post-injection. Liver, lungs, spleen, and lymph nodes were aseptically removed, and single-cell suspensions were prepared in 0.02 M PBS by tissue mashing. The cells were washed with PBS and labeled with PerCP-Cy5.5-labeled $CD11c^+$ marker at room temperature for 30 min. Cells were washed and analyzed for $CD11c^+$ rhodamine 123^+ populations. Flow cytometric data were obtained using a BD LSR Fortessa-Cell Analyzer Flow Cytometer (BD Biosciences, USA) and analyzed with FlowJo software (Tree Star).

Fluorometry-Based Analysis of the Intracellular Distribution of Liposomes. After incubation with liposomes at various time points, the cells were washed twice with phosphate buffered saline-calcium magnesium glucose (PBS-CMG)(137 mM NaCl, 2.7 mM KCl, 1.5 mM K_2HPO4, 8.1 mM Na_2HPO4, 0.4 mM $CaCl_2$, 0.4 mM $MgCl_2$, 5 mM glucose, pH 7.4) and incubated for 5 min at 37 °C with 1.5 mL of PBS containing 3 mM EDTA. The cells were dislodged and diluted in PBS. Corrected fluorescence excitation spectra (∼ex 395−465 nm, 1.8 nm bandwidth) were measured at 510 nm emission with a wide (4.5 nm) emission bandwidth using a PerkinElmer, LS-55. For calibration of pyranine quenching by DPX, liposomes were diluted to 50 mM in PBS, and fluorescence was measured. Fluorescence units are expressed as photon counts per second. Cells were stimulated with a pyranine-labeled liposome, harvested, and washed two times in PBS, and the fluorescence intensity associated with the cells was recorded at 405 and 450 nm by fluorometry. The fluorescence associated with the same number of cells incubated with respective empty liposomes was subtracted from that associated with cells incubated with fluorescence-containing liposomes for the elimination of autofluorescence. To determine the pH of the site occupied by the differentially charged liposomes indicating the intracellular fate of liposomes, the fluorescence emission ratio at excitation wavelengths of 450 and 405 nm was calculated.[21]

Statistical Analysis. Data are represented as the mean ± standard error of mean (SEM). One-way analysis of variance (ANOVA) and Tukey's multiple comparisons post-test were used for the analysis of data using Prism-Graphpad version 5.0 (Graph pad Software, v.5.0, San Diego, CA). p values of <0.05 were considered to be statistically significant.

RESULTS

Characterization of Lipid Particles. To Investigate the role of surface charge on the liposomes regulating DC-

https://doi.org/10.1021/acsomega.3c07814
ACS Omega 2024, 9, 29175−29185

i)

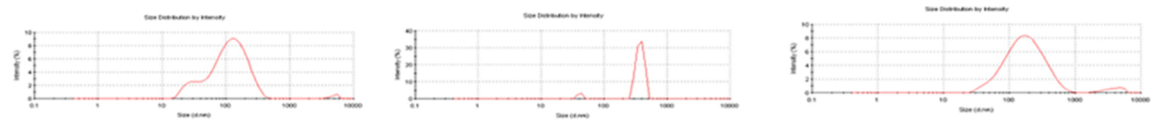

ii)

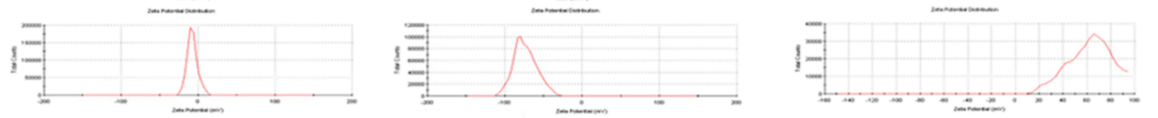

iii)

Liposomal Composition	Zeta Potential (mV)	Size (nm)	PDI
DSPC-Cholesterol	-6.17 ± 1.01	312.08 ± 24.08	0.47 ± 0.79
DSPC-Cholesterol-Phosphatidic Acid	-63.11 ± 7.42	414.2 ± 94.01	0.36 ± 0.74
DSPC-Cholesterol-Stearylamine	56.03 ± 3.65	212.0 ± 7.58	0.39 ± 0.21

iv)

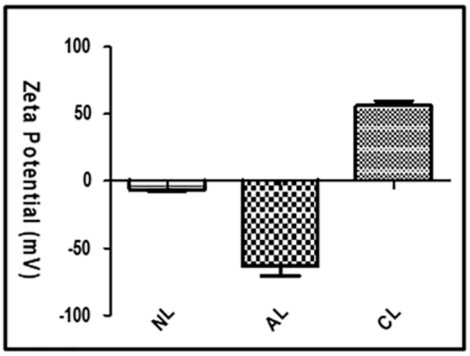

v)

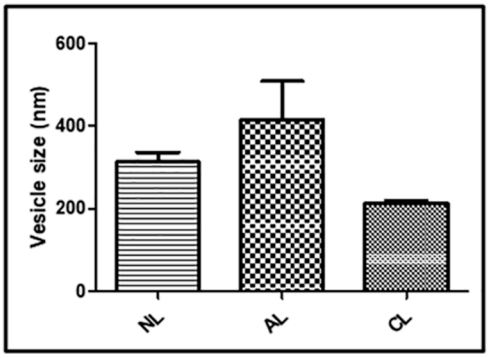

Figure 2. Physicochemical properties of differentially charged liposomes. The neutral, negatively, and positively charged liposomes were made with DSPC and cholesterol or DSPC, cholesterol, and either PA or SA, respectively (for details, see the Material and Method section). DLS plot of liposomal (i) size and (ii) zeta potential values in 0.01 M PBS. (iii) Tabular and (iv,v) graphical representation of zeta potential, size, and PDI of differentially charged liposomal formulations. Data represents mean ± SEM; n = 3−5.

mediated immune responses, we synthesized liposomes using lipids with different charging molecules and performed in vitro characterization. The liposome vehicles were prepared using a neutral lipid DSPC (zwitterionic) and cholesterol (helper lipid) to which a cationic molecule, stearylamine (SA, positively charged), or an anionic molecule PA (negatively charged) was introduced. Using the lipid thin film method, we synthesized DSPC−cholesterol (Chol)-based differentially charged liposomes composed of DSPC and cholesterol (7:2 molar ratio) neutral, DSPC−cholesterol−SA (7:2:2 molar ratio) cationic, and DSPC−cholesterol−PA (7:2:2 molar ratio) anionic liposomes (ALs) (Figures 1 and 2). Differential light scattering (DLS) method of characterization showed that DSPC-based cationic, anionic, and neutral liposomes (NLs) were 212 ± 7.58, 414.2 ± 94.01, 312.08 ± 24.08 nm in diameter with a PDI of 0.39 ± 0.21, 0.36 ± 0.74, 0.47 ± 0.79, respectively (Figure 2i,iii,v). Due to the presence of a tertiary amino group in DSPC−Chol−SA, these liposomes exhibit a zeta potential value of 56.03 ± 3.65 mV, whereas DSPC−Chol−PA showed a net negative zeta potential (−63.11 ± 7.42 mV) due to the phosphate group and a net neutral zeta value (−6.17 ± 1.01 mV) on DSPC−Chol liposomes due to the masking of charge for zwitterionic form of lipids (Figure 2ii,iv).

Phenotypic Maturation of BMDCCs Dependent on Liposomal Surface Charge. Premature DCs internalize pathogens or foreign particles in the peripheral organs and blood, then migrate to draining lymphoid tissue, where they undergo morphological changes with increased expression of surface molecules such as CD86, CD83, CD80, CD40, and MHC-II.[22] This symbolizes DC maturation for activation of T cells.[23] To understand the maturation effect of liposomes on DCs' cell surface, expression of costimulatory molecules (CD40 and CD86) was determined using flow cytometry (Figure 3). Compared to unstimulated DCs, LPS-treated cells exhibited a significant increase in CD86 expression (Figure 3b). Additionally, DCs stimulated with differently charged liposomes, particularly cationic and neutral ones, showed significant upregulation of CD86 compared with that in the control with only media. Interestingly, the addition of MPL to these liposomes significantly induced CD86 expression compared to that of the respective liposome stimulation alone. Similarly, CD40 expression reflected the CD86 pattern with LPS stimulation, significantly upregulating the expression level compared to that in the media control (Figure 3c). Furthermore, CLs, while showing a small elevation in CD40 expression when compared to that in the control with medium, exhibited significantly higher CD40 expression than anionic and NLs. The addition of MPL to the differently charged liposomes notably upregulated CD40 expression compared with that in DCs stimulated with respective charged liposomes alone. More interestingly, MPL-adjuvanted CLs significantly enhanced CD40 expression compared to that in adjuvanted anionic and NLs (Figure 3c). This elevation of CD40 expression with adjuvanted CLs though higher than that with MPL alone was, however, not significant.

https://doi.org/10.1021/acsomega.3c07814
ACS Omega 2024, 9, 29175−29185

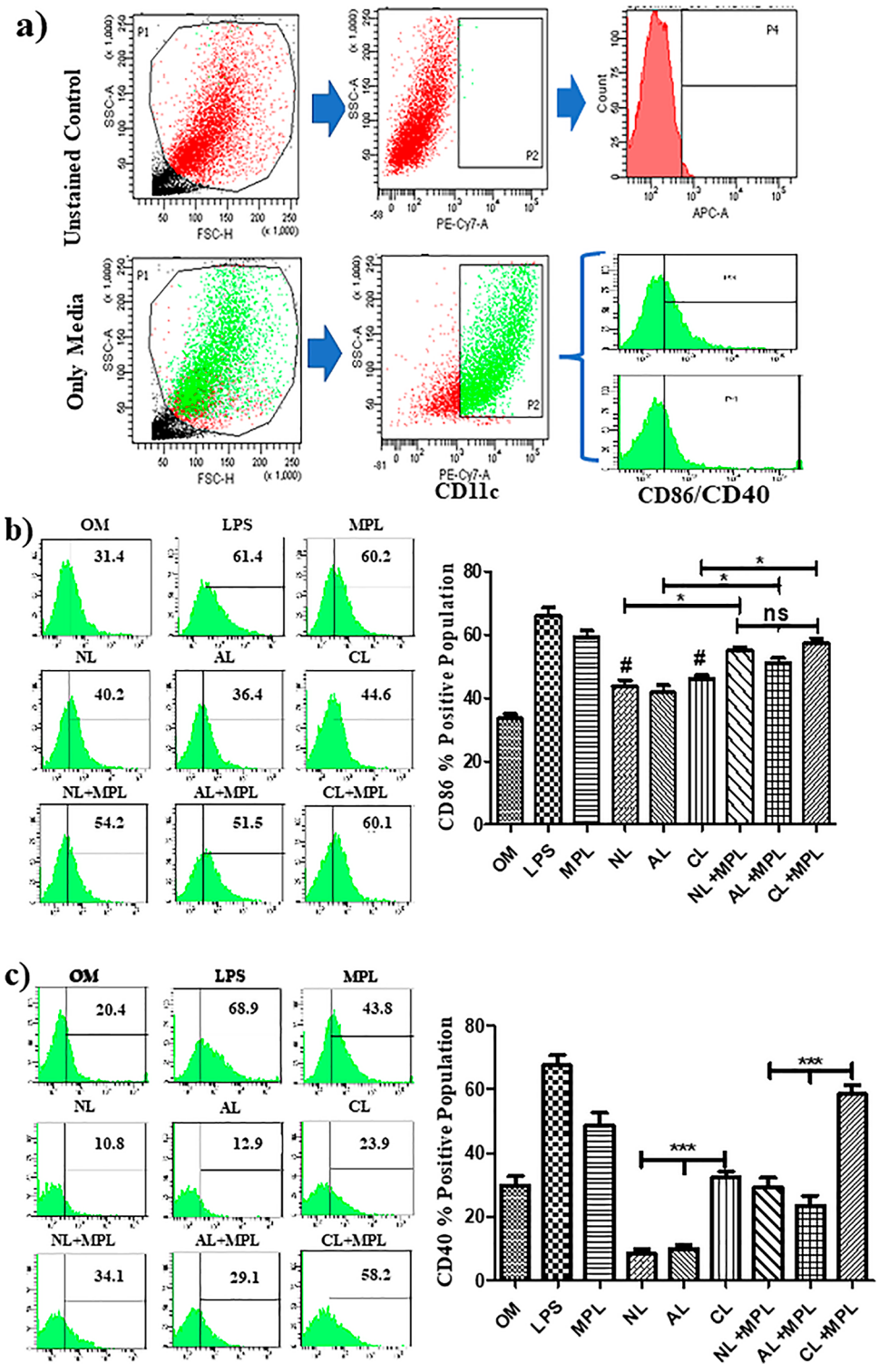

Figure 3. Effect of differentially charged liposomes (alone or with adjuvant) on BMDCs' maturation. Cultured BMDCs (day 6) were stimulated with only media, LPS (1 μg/mL), MPL-TDM (100 ng/mL), s ALs, NLs, and CLs (100 μM final liposome concentration for differentially charged liposomes) for 24 h. (a) Gating strategy for FACS analysis of stimulated DCs assessing the expression of the costimulatory molecules (CD86 and CD40). Prior to gating on the chosen markers for the investigation, CD11c+ cells were gated. (b,c) Cells were immunoassayed with fluorescently labeled antibodies against CD11c as a DC marker and measured for surface expression of the costimulatory molecules (b) CD86 and (c) CD40 by flow cytometry (data inside histogram plot represent percent positive population). Corresponding graph in the right panel summarizes percent positive population of three different experiments. #$p < 0.05$ (compared to untreated control), *$p < 0.05$, ***$p < 0.001$ analyzed by one-way ANOVA, followed by Tukey's multiple comparison test. ns- not significant.

Liposome-Induced Cytokine Production Substantiates Activation of BMDCs. The initial step in initiating an immunological response involves activating APCs, characterized by the increased production of key molecules such as TNF-α, IL-6, IL-1b, IL-12, and NO. Therefore, we investigated the activation capacity of the liposomal formulations on DCs.

https://doi.org/10.1021/acsomega.3c07814
ACS Omega 2024, 9, 29175−29185

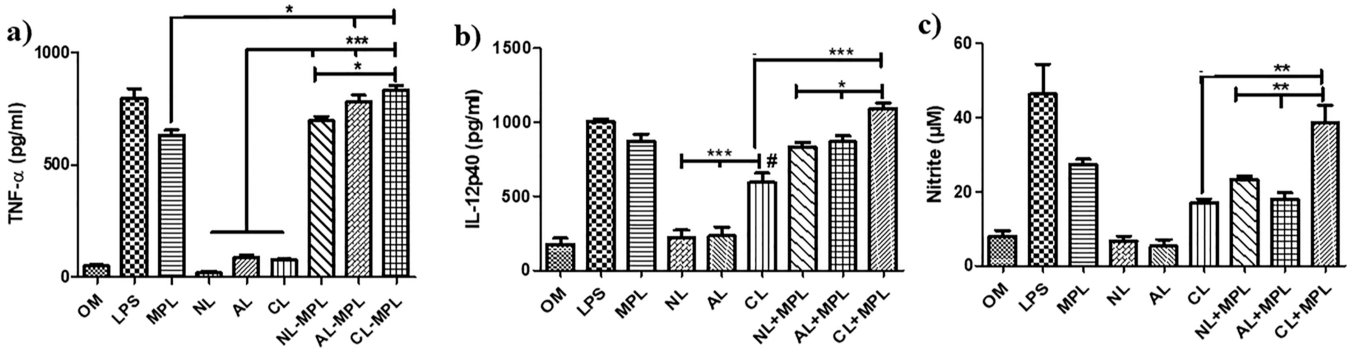

Figure 4. Immunostimulation of DCs following stimulation with differently charged liposomes alone or in combination with an adjuvant. Cultured BMDCs (day 6) were stimulated with only media, LPS (1 μg/mL), MPL (100 ng/mL), NLs, ALs and CLs (100 μM liposome concentration) for 48 h. Stimulated DC culture supernatants were removed for quantification of (a) TNF-α, (b) IL-12p40, and (c) NO production. Data represent triplicate mean ± standard error (SE) #$p < 0.05$ (compared to untreated control), *$p < 0.05$, **$p < 0.01$, ***$p < 0.001$ analyzed by one-way ANOVA, followed by Tukey's multiple comparison test.

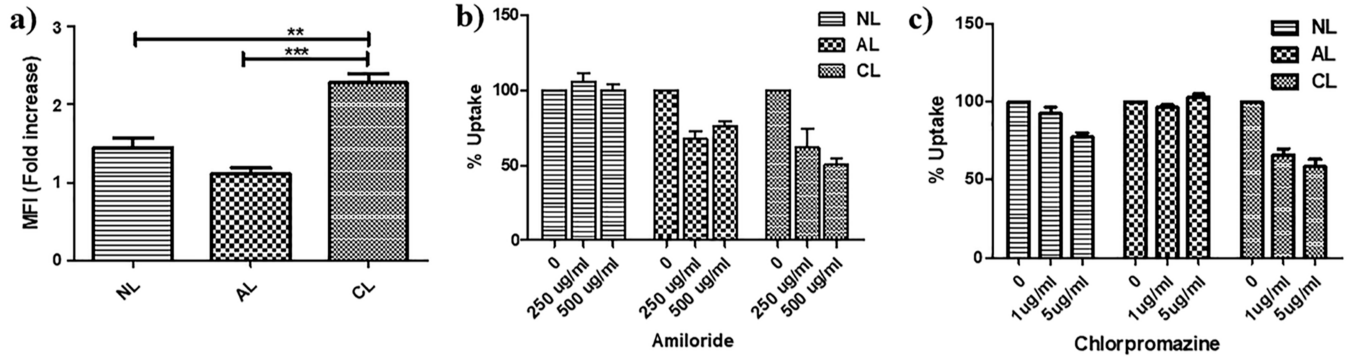

Figure 5. Fluorescence-activated cell sorter analysis of the cellular uptake mechanism of differentially charged liposomes (neutral, anionic, and cationic) on BMDCs in the presence or absence of inhibitors. (a) Uptake of liposomes, which were labeled with rhodamine 123, measured by flow cytometry after incubation of BMDCs with liposomes. Effect of (b) amiloride and (c) chlorpromazine on the uptake of different liposomes into BMDCs. The cells were incubated with amiloride or chlorpromazine for 30 min or 1 h, respectively, before addition of liposomes. After the incubation, the cells were washed three times with buffer to remove the liposomes bound to the surface of the cells. The percent uptake is expressed as the percentage of the mean fluorescence in the absence of inhibitors as control. Values are the mean ± SEM of at least three different experiments. **$p < 0.01$, ***$p < 0.001$ analyzed by one-way ANOVA, followed by Tukey's multiple comparison test.

Our observations revealed that treating DCs with LPS led to a substantial upregulation in the production of pro-inflammatory molecules, TNF-α, IL-12, and NO. It is worth mentioning that the stimulation of DCs with liposomes alone did not induce any substantial TNF-α production (Figure 4a). However, when DCs were stimulated with CLs, there was a noteworthy enhancement in the production of IL-12p40 and NO. This amplification in IL-12p40 and NO production was not only significantly higher than the only media control but also exceeded the response observed with anionic and NLs (Figure 4b,c).

In order to enhance the effectiveness of these particulate liposome formulations, we introduced MPL as an adjuvant and assessed the resulting cytokine and NO production by DCs. Our findings demonstrated that when charged liposomal formulations were combined with MPL, they significantly upregulated the production of TNF-α, IL-12, and NO in stimulated mouse DCs compared to that in the control with only media(Figures 3b and 4). The adjuvanted cationic liposomal formulation significantly upregulated TNF-α (Figure 4a), IL-12, (Figure 4b) and NO (Figure 4c) production, when compared to their negative and neutral counterparts. These results thus indicate the superior induction of DCs when CLs are mixed with MPL, which may play a major role in the enhancement of antigen presentation along with activation of T cell immunity with antigenic formulations.

Cellular Entrance Mechanism of Differentially Charged Liposomes. To understand the cellular entrance mechanism followed by differentially charged liposomes in BMDCs, we prepared rhodamine123 (aqueous-phase marker)-labeled liposomes and measured the uptake through fluorescence-activated cell sorter analysis. We observed that the uptake of CLs by the DCs was 1.5- and 2.0-fold higher when compared to that of neutral and ALs, respectively (Figure 5a).

We then investigated the effects of two cellular entrance pathway inhibitors, amiloride for macropinocytosis and chlorpromazine for clathrin-mediated endocytosis (Figure 5b,c). In the presence of 500 mol/L amiloride, the uptake of anionic and CLs by DCs was inhibited by 24 and 55%, respectively, whereas in the case of NL, no such effect was observed (Figure 5b). On the other hand, chlorpromazine (5 μg/mL) reduced the cellular uptake of neutral and CLs by 23 and 43%, respectively, while ALs had no such measurable effect (Figure 5c). These findings therefore demonstrate that CLs are substantially more readily taken up by both macropinocytosis and endocytosis pathways for processing within DCs than the other conventional liposomes.

https://doi.org/10.1021/acsomega.3c07814
ACS Omega 2024, 9, 29175−29185

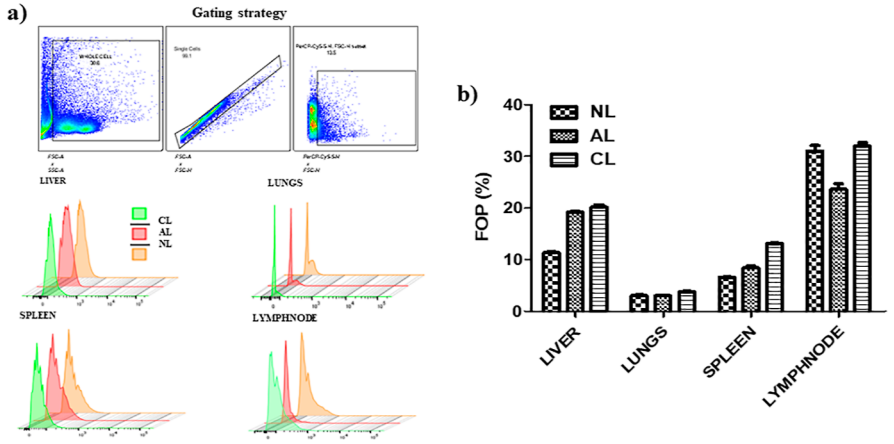

Figure 6. Exploration of in vivo uptake patterns of liposomes with varying charges (neutral, anionic, and cationic) by CD11c+ DCs across diverse organs using fluorescence-activated cell sorting. Single-cell suspensions from the liver, lungs, spleen, and lymph nodes of BALB/c mice ($n = 3$) were analyzed after intravenous injection with rhodamine-123-labeled liposomes for 18−24 h to examine the uptake of labeled liposomes by CD11c+ cells across these organs (see details in the "Methods" section). (a) Representation of the gating strategy employed for assessing the uptake of liposomes by CD11c+ DCs. Adjacent histograms depict the representative plots illustrating the uptake of differentially charged (CL, AL, and NL) labeled liposomes in various mouse organs. CL:green histogram, AL: red, and NL: brown. (b) Bar graph representing CD11c+ and rhodamine 123+ cells across different organs. FOP-frequency of parent (%). Values are the mean FOP ± SEM of at least three different experiments.

It has long been known that the relationship between in vitro optimization and in vivo effectiveness of vaccines is noticeably poor. This is primarily due to the complicated nature of the in vivo environment, which introduces complexity that in vitro studies do not completely represent.[24] Therefore, to correlate in vitro uptake of liposomes by DCs in vivo, rhodamine 123 liposomes were injected intravenously (i.v.) into BALB/c mice (80 μg/animal), and the biodistribution of differentially charged liposomes in various organs (like liver, lungs, spleen, and lymph nodes) was assessed. Presence of liposomal fluorescence signal in DCs residing in these organs indicates efficient uptake and biodistribution of liposomes in vivo. While the uptake of differentially charged liposomes varied in lymph nodes, spleens, and livers, positively charged liposomes, interestingly, exhibited the highest uptake (Figure 6a,b).

Modulation of the Intracellular Environment inside BMDCs after Liposomal Uptake. According to recent research, DCs display a delayed process of acidification and endolysosome maturation that limit lysosomal proteases' activity and slow down the degradation of antigens.[25] Antigens entrapped in liposomes can therefore be delivered to intracellular compartments for complexation with MHC-I molecules and presentation to CD8+ T cells while being protected from excessive degradation inside the APCs.[26] Earlier reports have demonstrated that amine-functionalized moieties are identified for their buffering capacities at a lower pH (basic pH value). Thus, we envisaged that stearylamine-bearing DSPC CLs when taken up by DCs may interfere with the modifications of the destined compartments' intracellular environment.[27] To reveal the intracellular activities of liposomes and to establish the pH of the occupied intracellular compartments, we used pyranine as an indicator and measured the fluorescence emission ratio at excitation wavelengths of 450 and 405 nm as described.[21] Fluorescence emission spectra from pyranine exhibit two distinct peaks at these two excitation wavelengths. The strength of the 450 nm peak is particularly sensitive to pH and decreases to zero at a low pH (6.0). When the pH falls below 6.0, the intensity of the latter peak at 405 nm increases somewhat. As a result, a greater intensity at 405 nm shows the presence of pyranine in acidic compartments, whereas a higher intensity at 450 nm indicates the presence of pyranine in neutral compartments.

BMDCs when pulsed with pyranine-labeled NLs, ALs, and CLs, the measured arbitrary unit (AU) values signify the efficient internalization of these liposomal formulations by DCs (Table 1). We observed that both NLs and ALs showed lower AU values at 450 nm and higher AU values at 405 nm, indicating the acidified compartmentalization of neutral and anionic lipid particles (most probably in lysosomal compartments). Interestingly, we found that CLs exhibited higher AU at 450 nm and lower at 405 nm, indicating the location of particles in organelles having lower pH (neutral to near-neutral compartments). Furthermore, greater fluorescence intensity, i.e., higher AU value in BMDCs with pyranine-labeled CLs, indicates that DCs took up DSPC−Chol−SA bearing positively charged liposomes much more efficiently than neutral and anionic ones.

Table 1. Uptake of Fluorescently Labeled Liposomes by BMDCs[a]

liposomal formulations	405 nm (AU)	450 nm (AU)
pyranine-labeled DSPC−Chol	207.52[b]	185.95
pyranine-labeled DSPC−Chol−PA	154.88	120.42
pyranine-labeled DSPC−Chol−SA	319.21	420.74

[a]Uptake of fluorescently labeled differentially charged (neutral, anionic, and cationic) liposomes by BMDCs. BMDCs were incubated with pyranine-labeled differentially charged liposomes for 18 h at 37 °C in a CO_2 incubator. After incubation period, the BMDCs were washed to remove the excess pyranine attached on the surface of liposomes, and the fluorescent intensity was measured at excitation wavelengths of 405 and 450 nm. Data demonstrate that one of five experiments yielding similar results. CL-cationic liposome; AL-anionic liposome; NL-neutral liposome. [b]Fluorescence intensity in AU.

DISCUSSION

Optimizing the physicochemical characteristics and adjuvanticity of vehicles without cargo molecules is one of the key

https://doi.org/10.1021/acsomega.3c07814
ACS Omega 2024, 9, 29175−29185

aspects for efficient immune modulation with liposomal formulations.[28] Physicochemical characteristics such as size, composition, and charge determine the fate (recognition and uptake process) of the formulations within APCs and their impact on protective immunological responses.[29−31] In this study, we delved into the critical aspects of optimizing liposomal formulations for efficient immune modulation, particularly focusing on the liposomal charge and adjuvanticity. We observed that liposomes significantly affected the immunostimulatory activity of DCs, which is related to the surface charge of the liposomes. The addition of an adjuvant MPL, to all the formulations (neutral, anionic, and cationic) improved the immunostimulatory activity of the three formulations, with highest improvement in DC maturation and stimulation seen by CLs. Further, we confirmed that macropinocytosis is the major route of uptake for positively charged liposomes along with a certain amount following the endocytic route. The current study further indicates that CLs are preferentially destined to the neutral to near-neutral compartments (most likely the cytosol) for their further processing after being taken up by DCs, whereas NLs and ALs are transported to the acidic compartments. These findings offer valuable insights into the development of effective vaccines for a range of critical diseases.

We prepared differentially charged DSPC liposomes with lipids bearing varying charges and characterized them based on their size and charge. The ALs composed of DSPC/PA were of the largest size, having a size of almost 414 nm. The CLs and NLs composed of DSPC/Chol/SA and DSPC/Chol, respectively, were in a size range of 200−300 nm. Beyond the charge dependency, the structural and compositional aspects of liposomes also significantly impact their ability to stimulate DCs. Using distinctly charged liposomes bearing the same hydrocarbon chains and headgroup functionalities (DSPC) herein, we demonstrate that liposomes bearing a net positive charge induced a higher level expression of costimulatory molecules of CD40 and CD86 in BMDCs. Upregulated expression of costimulatory molecules like CD40, CD58, CD80, and CD86 indicates the activation of DCs and triggers their transition from antigen-capturing to antigen-presenting DCs.[32] The zwitterionic and negatively charged forms, however, induced lower levels of costimulatory molecular expression compared to that of the cationic form of DSPC liposomes. The net positive electric charge of CLs supports favorable interaction with the negatively charged cell membrane. The interaction between APCs and lipid head groups is a crucial aspect influencing the activation of DCs.[13,33] This interaction might involve specific signaling pathways or molecular mechanisms that trigger the activation of DCs upon exposure to lipid head groups. Incorporating a helper lipid during liposome formation offers notable benefits.[34,35] It reduces endothelial uptake, improving the circulation time. Additionally, it modifies the surface charge, influencing interactions with biological entities. Furthermore, it enhances liposome stability, which is critical for effective payload delivery. Additionally, past research has demonstrated an increase in costimulatory molecules and cytokine production upon introducing cationic particles to DCs.[36−38] Moreover, liposomes composed of liquid disordered lipids outperform those containing solid ordered phase lipids in terms of antigen cross-presentation, altering the fate of carrier molecules enclosed within the liposomes.[39,40] Our research, in conjunction with these earlier studies, suggests that the diverse use of lipid molecules and charges in liposome production plays a pivotal role in activating APCs.

We therefore sort to exploit the effect of the variably charged liposomes alone and along with adjuvants on the multiple arms of the immune system. Combinatorial adjuvant strategies that target multiple divisions of the immune system at the same time may lead to enhancing the development of next-generation vaccines.[8,41,42] CD40 and CD86, being key immune costimulatory molecules, were studied. Herein, we report that liposomal formulations, especially cationic, initiate TLR-4 signaling, leading to costimulatory molecule expression like that of CD40/CD86, which is enhanced significantly with incorporation of MPL into the formulation. NO, TNF-α (tumor necrosis factor-alpha), and IL-12 (interleukin-12) play pivotal roles in the immune system, underscoring the significance of monitoring their levels. When administered independently, NLs and ALs did not stimulate the production of TNF-α, IL-12, or NO. However, upon the addition of MPL to these formulations, there was a noteworthy enhancement in the levels of these molecules. Intriguingly, cationic liposomal formulations demonstrated significant upregulation of TNF-α, IL-12, and NO levels even when used as standalone treatments. Furthermore, the addition of MPL substantially amplified these levels, illustrating a synergistic effect. However, it is important to note that BMDCs when stimulated using liposomes alone were not able to induce a significant level of TNF-α production, indicating a role of adjuvant in TNF-α production. The enhanced stimulatory effect observed with CLs, either alone or in conjunction with MPL, could potentially be attributed to the activation of the TLR signaling pathways. Existing research has established that subunit vaccines incorporating TLR adjuvants primarily target DCs, a critical cell type orchestrating immune responses through TLR signaling activation, including pathways like nuclear factor kappa B (NF-κB), myeloid differentiation primary response 88 (MyD88), and TIR-domain-containing adaptor-inducing beta interferon (TRIF).[43,44]

In this context, it has been reported that cationic lipids induce NF-κB signaling, thereby activating DCs and prominently stimulating the MyD88 pathway.[38,45] This may shed light on why the production of CD40, IL-12, and NO is not significantly elevated with ALs and NLs when used alone in DCs. Electrostatic interactions between ligands and receptors often play a pivotal role in TLR signaling.[46] The limited charge compatibility of ALs and NLs might impede their effective engagement with TLRs, resulting in reduced signaling and subsequent immune response activation.

Previous research has suggested that DCs take up and process molecules from the extracellular environment, triggering their maturation and subsequent migration to lymphoid organs. This ultimately enables DCs to facilitate immunostimulatory activities.[47,48] Understanding the cellular uptake and intracellular destiny of vesicles is pivotal in the study of delivery vehicles for targeted therapy under various disease conditions. This knowledge is essential for the development of a delivery system that is both safe and efficacious.[49−52] For the therapy to be effective, these vesicles need to be taken up by the target cells and navigate their intracellular fate. Factors influencing cellular uptake include the vesicle size, surface charge, and targeting ligands. Intracellular fate involves processes such as endosomal escape, release of therapeutic cargo, and localization within specific cellular compartments.

https://doi.org/10.1021/acsomega.3c07814
ACS Omega 2024, 9, 29175−29185

We found that CLs show the highest uptake by DCs in comparison to NLs and ALs. In all mammalian cell types including DCs, polar or charged biomolecules are internalized or taken up by a form of active transport pathway like phagocytosis, endocytosis, macropinocytosis, phagocytosis, and receptor-mediated endocytosis.[53] Particles with diameters > 750 nm are mostly taken up by phagocytosis, whereas smaller particles with diameters ranging from a few nanometers to a few hundred nanometers are picked up by pinocytosis or macropinocytosis.[54] Additionally, it was reported earlier that smaller liposomes are readily taken up by APCs and induce type 1 T helper (Th1) type of immunological responses, whereas larger liposomes induce type 2 T helper (Th2) responses.[40] Given that our liposomes fall within the 200 to 400 nm range, they are most likely to be taken up through micropinocytosis or endocytosis processes. To analyze the uptake of differentially charged liposomes by DCs, we employed two inhibitors: amiloride, a macropinocytosis inhibitor, and chlorpromazine, an endocytosis inhibitor. Remarkably, NLs showed no discernible effect with amiloride inhibition, suggesting the absence of macropinocytosis involvement. However, partial changes were noted with chlorpromazine inhibition, indicating a possible role of endocytic uptake. In contrast, ALs demonstrated evident uptake, primarily through macropinocytosis. Notably, the uptake of CLs was significantly inhibited by both amiloride and chlorpromazine, suggesting a complex uptake mechanism involving both macropinocytosis and endocytosis pathways. Additionally, the in vitro uptake pattern of differentially charged liposomes corelates with in vivo biodistribution findings. Herein, we report that while the uptake of differentially charged liposomes varied in lymph nodes, spleens, and livers, positively charged liposomes, interestingly, exhibited the highest uptake.

We next examined the intracellular fate of liposomes inside DCs using pyranine-labeled liposomes, a pH-sensitive dye to precisely identify the delivery site. This dye exhibits two peaks (at 405 and 450 nm) depending upon the pH of the site occupied by the liposomes. The higher intensity value at 405 nm peak indicates localization of liposomes at acidified compartment, whereas greater intensity at 450 nm indicates the presence of liposomes at neutral compartments.[21] Herein, we report that NLs and ALs were transported to the acidic compartments, perhaps lysosomal compartments. The lysosomal compartment is crucial in the major histocompatibility complex (MHC) class II pathway as it is involved in the degradation and processing of exogenous antigens into peptides that can be loaded onto MHC class II molecules for presentation to CD4+ T cells. Interestingly, we found that CLs were carried to neutral or nearly neutral pH containing (AU value of 450 > 405 nm) compartments, most likely the cytosol of DCs. Due to the presence of cationic moiety in our liposomes when they come in contact with an endolysosomal compartment, these liposomes may undergo interaction with anionic endosomal membrane. This interaction possibly induces mixing of lipids between the liposomes and the endosomal membrane, thereby promoting cytosolic localization and leading to the subsequent release of the cargo molecules into the cytosol.[3] Herein, we suggest that directing the lipid vesicles to endolysosomal compartments has the potential to extend the cytosolic delivery of antigens entrapped in CLs. Our previous studies also report similar findings,[55] which are also supported by others.[27,49,56,57] Consequently, it can induce CD4+ T cell stimulation through conventional presentation pathways, but interestingly, it might also facilitate cross-presentation, leading to the priming of CD8+ T cells. To address these concerns, future investigations should be directed to examine the effect of antigen-entrapped differentially charged liposomal formulations and their intracellular processing and presentation inside major APCs (in both DCs and macrophages).

CONCLUSIONS

In conclusion, our research offers crucial insights into leveraging liposomes based on DSPC with differing charges to activate and immunostimulate DCs, while elucidating their intracellular behavior. Notably, CLs display markedly heightened stimulation potential and exhibit a clear preference for uptake and endolysosomal routing within DCs compared to their neutral and anionic counterparts. These findings underscore the significant promise of CLs as a compelling strategy for future investigations in the strategic design of vaccine delivery platforms, offering favorable characteristics in activation, uptake, and targeted delivery.

AUTHOR INFORMATION

Corresponding Author

Nahid Ali − *Infectious Diseases and Immunology Division, CSIR-Indian Institute of Chemical Biology, Kolkata 700032, India;* orcid.org/0000-0003-1932-5916; Phone: 91-33-2473-3491; Email: nali@iicb.res.in; Fax: 91-332473-0284

Authors

Mithun Maji − *Infectious Diseases and Immunology Division, CSIR-Indian Institute of Chemical Biology, Kolkata 700032, India;* Present Address: Department of Botany, Dinabandhu Andrews College, 54, Raja S.C. Mullick Road, Baishnabghata, Garia, Kolkata-700084

Sneha Ghosh − *Infectious Diseases and Immunology Division, CSIR-Indian Institute of Chemical Biology, Kolkata 700032, India;* Present Address: Department of Biochemistry, University of Calcutta, Kolkata, India.

Nicky Didwania − *Infectious Diseases and Immunology Division, CSIR-Indian Institute of Chemical Biology, Kolkata 700032, India*

Complete contact information is available at: https://pubs.acs.org/10.1021/acsomega.3c07814

Author Contributions

M.M. and N.A. conceived the study, designed the experiments, analyzed the data, and wrote the manuscript. M.M., N.D., and S.G. performed and optimized the experiments, prepared figures, and contributed reagents. All authors critically revised and approved the manuscript.

Notes

The authors declare no competing financial interest.

ACKNOWLEDGMENTS

We would like to thank our funding agencies such as Global Challenges Research Fund under the grant agreement, 'A Global Network for Neglected Tropical Diseases'. Grant number MR/P027989/1, India, Indian Council of Medical Research and Council of Scientific and Industrial Research, India, and Sir J.C. Bose Fellowship grant number SB/S2/JCB-

https://doi.org/10.1021/acsomega.3c07814
ACS Omega 2024, 9, 29175−29185

21/2015, India. The authors would also like to appreciate Biorender.com for their software support.

REFERENCES

(1) Amanna, I. J.; Slifka, M. K. Successful Vaccines. *Curr. Top. Microbiol. Immunol.* **2018**, *428*, 1−30.
(2) Nam, J.; Son, S.; Park, K. S.; Moon, J. J. Modularly Programmable Nanoparticle Vaccine Based on Polyethyleneimine for Personalized Cancer Immunotherapy. *Adv. Sci.* **2021**, *8* (5), 2002577.
(3) Gandek, T. B.; van der Koog, L.; Nagelkerke, A. A Comparison of Cellular Uptake Mechanisms, Delivery Efficacy, and Intracellular Fate between Liposomes and Extracellular Vesicles. *Adv. Healthcare Mater.* **2023**, *12*, No. e2300319.
(4) O'Hagan, D. T. Recent Developments in Vaccine Delivery Systems. *Curr. Drug Targets: Infect. Disord.* **2001**, *1*, 273−286.
(5) Chatzikleanthous, D.; O'Hagan, D. T.; Adamo, R. Lipid-Based Nanoparticles for Delivery of Vaccine Adjuvants and Antigens: Toward Multicomponent Vaccines. *Mol. Pharmaceutics* **2021**, *18* (8), 2867−2888.
(6) Bergmann-Leitner, E. S.; Leitner, W. W. Adjuvants in the Driver's Seat: How Magnitude, Type, Fine Specificity and Longevity of Immune Responses Are Driven by Distinct Classes of Immune Potentiators. *Vaccines* **2014**, *2*, 252−296.
(7) Facciolà, A.; Visalli, G.; Laganà, A.; Di Pietro, A. An Overview of Vaccine Adjuvants: Current Evidence and Future Perspectives. *Vaccines* **2022**, *10* (5), 819.
(8) Krasnopolsky, Y.; Pylypenko, D. Licensed Liposomal Vaccines and Adjuvants in the Antigen Delivery System. *BioTechnologia* **2022**, *103* (4), 409−423.
(9) Schwendener, R. A. Liposomes as Vaccine Delivery Systems: A Review of the Recent Advances. *Ther. Adv. Vaccines* **2014**, *2* (6), 159−182.
(10) Wang, N.; Chen, M.; Wang, T. Liposomes Used as a Vaccine Adjuvant-Delivery System: From Basics to Clinical Immunization. *J. Controlled Release* **2019**, *303*, 130−150.
(11) Kotsias, F.; Cebrian, I.; Alloatti, A. Antigen Processing and Presentation. *Int. Rev. Cell Mol. Biol.* **2019**, *348*, 69−121.
(12) Nagy, N. A.; Castenmiller, C.; Vigario, F. L.; Sparrius, R.; van Capel, T. M.; de Haas, A. M.; van Kooyk, Y.; van Ree, R.; Tas, S. W.; Geijtenbeek, T. B. H.; Jiskoot, W.; Slütter, B.; de Jong, E. C. Uptake Kinetics Of Liposomal Formulations of Differing Charge Influences Development of *in vivo* Dendritic Cell Immunotherapy. *J. Pharm. Sci.* **2022**, *111* (4), 1081−1091.
(13) Wang, H.; Mehal, W.; Nagy, L. E.; Rotman, Y. Immunological Mechanisms and Therapeutic Targets of Fatty Liver Diseases. *Cell. Mol. Immunol.* **2021**, *18* (1), 73−91.
(14) Li, M.; Du, C.; Guo, N.; Teng, Y.; Meng, X.; Sun, H.; Li, S.; Yu, P.; Galons, H. Composition Design and Medical Application of Liposomes. *Eur. J. Med. Chem.* **2019**, *164*, 640−653.
(15) Ali, N.; Afrin, F. Protection of Mice against Visceral Leishmaniasis by Immunization with Promastigote Antigen Incorporated in Liposomes. *J. Parasitol.* **1997**, *83* (1), 70.
(16) Afrin, F.; Anam, K.; Ali, N. Induction of Partial Protection against Leishmania Donovani by Promastigote Antigens in Negatively Charged Liposomes. *J. Parasitol.* **2000**, *86* (4), 730.
(17) Afrin, F.; Ali, N. Adjuvanticity and Protective Immunity Elicited by Leishmania Donovani Antigens Encapsulated in Positively Charged Liposomes. *Infect. Immun.* **1997**, *65* (6), 2371−2377.
(18) Lee, K. D.; Nir, S.; Papahadjopoulos, D. Quantitative Analysis of Liposome-Cell Interactions *in vitro*: Rate Constants of Binding and Endocytosis with Suspension and Adherent J774 Cells and Human Monocytes. *Biochemistry* **1993**, *32* (3), 889−899.
(19) Inaba, K.; Inaba, M.; Romani, N.; Aya, H.; Deguchi, M.; Ikehara, S.; Muramatsu, S.; Steinman, R. M. Generation of Large Numbers of Dendritic Cells from Mouse Bone Marrow Cultures Supplemented with Granulocyte/Macrophage Colony-Stimulating Factor. *J. Exp. Med.* **1992**, *176* (6), 1693−1702.
(20) Mazumder, S.; Maji, M.; Ali, N. Potentiating Effects of MPL on DSPC Bearing Cationic Liposomes Promote Recombinant GP63 Vaccine Efficacy: High Immunogenicity and Protection. *PLoS Neglected Trop. Dis.* **2011**, *5* (12), No. e1429.
(21) Straubinger, R. M.; Papahadjopoulos, D.; Hong, K.; Straubinger, R. M.; Papahadjopoulos, D.; Hong, K. Endocytosis and Intracellular Fate of Liposomes Using Pyranine as a Probe. *Biochemistry* **1990**, *29* (20), 4929−4939.
(22) Liu, Y.; Jiao, F.; Qiu, Y.; Li, W.; Lao, F.; Zhou, G.; Sun, B.; Xing, G.; Dong, J.; Zhao, Y.; Chai, Z.; Chen, C. The Effect of Gd@C82(OH)22 Nanoparticles on the Release of Th1/Th2 Cytokines and Induction of TNF-α Mediated Cellular Immunity. *Biomaterials* **2009**, *30* (23−24), 3934−3945.
(23) Tenchov, R.; Bird, R.; Curtze, A. E.; Zhou, Q. Lipid Nanoparticles from Liposomes to MRNA Vaccine Delivery, a Landscape of Research Diversity and Advancement. *ACS Nano* **2021**, *15*, 16982−17015.
(24) Kranz, L. M.; Diken, M.; Haas, H.; Kreiter, S.; Loquai, C.; Reuter, K. C.; Meng, M.; Fritz, D.; Vascotto, F.; Hefesha, H.; Grunwitz, C.; Vormehr, M.; Hüsemann, Y.; Selmi, A.; Kuhn, A. N.; Buck, J.; Derhovanessian, E.; Rae, R.; Attig, S.; Diekmann, J.; Jabulowsky, R. A.; Heesch, S.; Hassel, J.; Langguth, P.; Grabbe, S.; Huber, C.; Türeci, Ö.; Sahin, U. Systemic RNA Delivery to Dendritic Cells Exploits Antiviral Defence for Cancer Immunotherapy. *Nature* **2016**, *534* (7607), 396−401.
(25) Blander, J. M. Regulation of the Cell Biology of Antigen Cross-Presentation. *Annu. Rev. Immunol.* **2018**, *36*, 717−753.
(26) Mantel, I.; Sadiq, B. A.; Blander, J. M. Spotlight on TAP and Its Vital Role in Antigen Presentation and Cross-Presentation. *Mol. Immunol.* **2022**, *142*, 105−119.
(27) Gao, J.; Ochyl, L.; Yang, E.; Moon, J. Cationic Liposomes Promote Antigen Cross-Presentation in Dendritic Cells by Alkalizing the Lysosomal PH and Limiting the Degradation of Antigens. *Int. J. Nanomed.* **2017**, *12*, 1251−1264.
(28) Nakhaei, P.; Margiana, R.; Bokov, D. O.; Abdelbasset, W. K.; Jadidi Kouhbanani, M. A.; Varma, R. S.; Marofi, F.; Jarahian, M.; Beheshtkhoo, N. Liposomes: Structure, Biomedical Applications, and Stability Parameters With Emphasis on Cholesterol. *Front. Bioeng. Biotechnol.* **2021**, *9*, 705886.
(29) Sheikholeslami, B.; Lam, N. W.; Dua, K.; Haghi, M. Exploring the Impact of Physicochemical Properties of Liposomal Formulations on Their *in vivo* Fate. *Life Sci.* **2022**, *300*, 120574.
(30) Pati, R.; Shevtsov, M.; Sonawane, A. Nanoparticle Vaccines against Infectious Diseases. *Front. Immunol.* **2018**, *9*, 2224.
(31) Tapia, D.; Reyes-Sandoval, A.; Sanchez-Villamil, J. I. Protein-Based Nanoparticle Vaccine Approaches Against Infectious Diseases. *Arch. Med. Res.* **2023**, *54*, 168−175.
(32) Alloatti, A.; Kotsias, F.; Magalhaes, J. G.; Amigorena, S. Dendritic Cell Maturation and Cross-Presentation: Timing Matters! *Immunol. Rev.* **2016**, *272*, 97−108.
(33) Vishvakrama, P.; Sharma, S. Liposomes: An Overview. *J. Drug Deliv. Therapeut.* **2014**, *4*, 47−55.
(34) Cheng, X.; Lee, R. J. The Role of Helper Lipids in Lipid Nanoparticles (LNPs) Designed for Oligonucleotide Delivery. *Adv. Drug Deliv. Rev.* **2016**, *99*, 129−137.
(35) Tseu, G. Y. W.; Kamaruzaman, K. A. A Review of Different Types of Liposomes and Their Advancements as a Form of Gene Therapy Treatment for Breast Cancer. *Molecules* **2023**, *28*, 1498.
(36) Pizzuto, M.; Bigey, P.; Lachagès, A. M.; Hoffmann, C.; Ruysschaert, J.-M.; Escriou, V.; Lonez, C. Cationic Lipids as One-Component Vaccine Adjuvants: A Promising Alternative to Alum. *J. Controlled Release* **2018**, *287*, 67−77.
(37) Tanaka, T.; Legat, A.; Adam, E.; Steuve, J.; Gatot, J. S.; Vandenbranden, M.; Ulianov, L.; Lonez, C.; Ruysschaert, J. M.; Muraille, E.; Tuynder, M.; Goldman, M.; Jacquet, A. DiC14-Amidine Cationic Liposomes Stimulate Myeloid Dendritic Cells through Toll-like Receptor 4. *Eur. J. Immunol.* **2008**, *38* (5), 1351−1357.

https://doi.org/10.1021/acsomega.3c07814
ACS Omega 2024, 9, 29175−29185

(38) Vangasseri, D. P.; Cui, Z.; Chen, W.; Hokey, D. A.; Falo, L. D.; Huang, L. Immunostimulation of Dendritic Cells by Cationic Liposomes. *Mol. Membr. Biol.* **2006**, *23* (5), 385−395.
(39) Christensen, D.; Henriksen-Lacey, M.; Kamath, A. T.; Lindenstrøm, T.; Korsholm, K. S.; Christensen, J. P.; Rochat, A.-F.; Lambert, P.-H.; Andersen, P.; Siegrist, C.-A.; Perrie, Y.; Agger, E. M. A Cationic Vaccine Adjuvant Based on a Saturated Quaternary Ammonium Lipid Have Different *in vivo* Distribution Kinetics and Display a Distinct CD4 T Cell-Inducing Capacity Compared to Its Unsaturated Analog. *J. Controlled Release* **2012**, *160* (3), 468−476.
(40) Tretiakova, D. S.; Vodovozova, E. L. Liposomes as Adjuvants and Vaccine Delivery Systems. *Biochem. (Moscow), Suppl. Ser.* **2022**, *16* (1), 1−20.
(41) O'Hagan, D. T.; Lodaya, R. N.; Lofano, G. The Continued Advance of Vaccine Adjuvants - 'We Can. Work It Out.'. *Semin. Immunol.* **2020**, *50*, 101426.
(42) Perrie, Y.; Mohammed, A. R.; Kirby, D. J.; McNeil, S. E.; Bramwell, V. W. Vaccine Adjuvant Systems: Enhancing the Efficacy of Sub-Unit Protein Antigens. *Int. J. Pharm.* **2008**, *364*, 272−280.
(43) Pulendran, B.; S Arunachalam, P.; O'Hagan, D. T. Emerging Concepts in the Science of Vaccine Adjuvants. *Nat. Rev. Drug Discovery* **2021**, *20* (6), 454−475.
(44) Pulendran, B.; Ahmed, R. Immunological Mechanisms of Vaccination. *Nat. Immunol.* **2011**, *12*, 509−517.
(45) Vaure, C.; Liu, Y. A Comparative Review of Toll-like Receptor 4 Expression and Functionality in Different Animal Species. *Front. Immunol.* **2014**, *5*, 316.
(46) Chen, Y.; Lin, J.; Zhao, Y.; Ma, X.; Yi, H. Toll-like Receptor 3 (TLR3) Regulation Mechanisms and Roles in Antiviral Innate Immune Responses. *J. Zhejiang Univ., Sci., B* **2021**, *22*, 609−632.
(47) Steinman, R. M.; Pack, M.; Inaba, K. Dendritic Cells in the T-Cell Areas of Lymphoid Organs. *Immunol. Rev.* **1997**, *156*, 25−37.
(48) Dudziak, D.; Kamphorst, A. O.; Heidkamp, G. F.; Buchholz, V. R.; Trumpfheller, C.; Yamazaki, S.; Cheong, C.; Liu, K.; Lee, H. W.; Park, C. G.; Steinman, R. M.; Nussenzweig, M. C. Differential Antigen Processing by Dendritic Cell Subsets *in vivo*. *Science* **2007**, *315* (5808), 107−111.
(49) Ignatius, R.; Mahnke, K.; Rivera, M.; Hong, K.; Isdell, F.; Steinman, R. M.; Pope, M.; Stamatatos, L. Presentation of Proteins Encapsulated in Sterically Stabilized Liposomes by Dendritic Cells Initiates CD8(+) T-Cell Responses *in vivo*. *Blood* **2000**, *96* (10), 3505−3513.
(50) Paramasivam, P.; Franke, C.; Stöter, M.; Höijer, A.; Bartesaghi, S.; Sabirsh, A.; Lindfors, L.; Arteta, M. Y.; Dahlén, A.; Bak, A.; Andersson, S.; Kalaidzidis, Y.; Bickle, M.; Zerial, M. Endosomal Escape of Delivered MRNA from Endosomal Recycling Tubules Visualized at the Nanoscale. *J. Cell Biol.* **2022**, *221* (2), No. e202110137.
(51) Sabnis, S.; Kumarasinghe, E. S.; Salerno, T.; Mihai, C.; Ketova, T.; Senn, J. J.; Lynn, A.; Bulychev, A.; McFadyen, I.; Chan, J.; Almarsson, O.⋯; Stanton, M. G.; Benenato, K. E. A Novel Amino Lipid Series for MRNA Delivery: Improved Endosomal Escape and Sustained Pharmacology and Safety in Non-Human Primates. *Mol. Ther.* **2018**, *26* (6), 1509−1519.
(52) Steinman, R. M.; Inaba, K.; Turley, S.; Pierre, P.; Mellman, I. Antigen Capture, Processing, and Presentation by Dendritic Cells: Recent Cell Biological Studies. *Hum. Immunol.* **1999**, *60* (7), 562−567.
(53) Foroozandeh, P.; Aziz, A. A. Insight into Cellular Uptake and Intracellular Trafficking of Nanoparticles. *Nanoscale Res. Lett.* **2018**, *13* (1), 339.
(54) Zhao, F.; Zhao, Y.; Liu, Y.; Chang, X.; Chen, C.; Zhao, Y. Cellular Uptake, Intracellular Trafficking, and Cytotoxicity of Nanomaterials. *Small* **2011**, *7* (10), 1322−1337.
(55) Maji, M.; Mazumder, S.; Bhattacharya, S.; Choudhury, S. T.; Sabur, A.; Shadab, Md.; Bhattacharya, P.; Ali, N. A Lipid Based Antigen Delivery System Efficiently Facilitates MHC Class-I Antigen Presentation in Dendritic Cells to Stimulate CD8+ T Cells. *Sci. Rep.* **2016**, *6* (1), 27206.
(56) Nakamura, T.; Moriguchi, R.; Kogure, K.; Shastri, N.; Harashima, H. Efficient MHC Class I Presentation by Controlled Intracellular Trafficking of Antigens in Octaarginine-Modified Liposomes. *Mol. Ther.* **2008**, *16* (8), 1507−1514.
(57) Miura, N.; Akita, H.; Tateshita, N.; Nakamura, T.; Harashima, H. Modifying Antigen-Encapsulating Liposomes with KALA Facilitates MHC Class I Antigen Presentation and Enhances Anti-Tumor Effects. *Mol. Ther.* **2017**, *25* (4), 1003−1013.

https://doi.org/10.1021/acsomega.3c07814
ACS Omega 2024, 9, 29175−29185